Advances in liquid crystal based devices for wavefront control and beamsteering

Steve Serati and Jay Stockley
Boulder Nonlinear Systems, Inc.
450 Courtney Way, #107
Lafayette, Colorado 80026

ABSTRACT

New devices and approaches are being developed for controlling beam direction and shape using liquid crystal based assemblies. This paper discusses recent advancements in these areas including improvements in zero-order diffraction efficiency, broadband wide field-of-regard steering, wavefront correction using in-line configurations and high average power handling.

Keywords: Liquid crystal phase modulators, optical tweezers, multi-spot beam steering

1. INTRODUCTION

Liquid-crystal spatial light modulators (SLMs) are capable of dynamically generating high-resolution phase masks. This capability is useful for steering the field of view of passive and active imaging systems,[1,2,3] providing spatially diverse links from a common aperture for multi-access free-space optical communications,[4,5] producing and manipulating multiple spots to function as agile laser tweezers,[6,7,8] as well as performing higher-order modal or zonal wavefront control for correcting[9,10,11,12] or simulating[13,14] atmospheric distortion. There are different requirements for each application, but the trend to improve efficiency and power handling, increase spectral range and operating speed, and develop compact, in-line configurations is beneficial for both wavefront control and beam steering.

Pixelated SLMs diffract light into higher orders, which reduces device efficiency and causes sidelobe interference. Therefore, it is desirable to maximize the zero-order efficiency of the modulator, which is directly related to the square of the fill factor. A technique that increases the fill factor of liquid crystal on silicon (LCoS) devices to nearly 100% has been developed and demonstrated. Its objective is to remove reflector discontinuities and smooth pixel-to-pixel phase transitions allowing the device to operate as a continuous deformable mirror. At each pixel, the phase modulator provides 0 to 2π of optical path difference (OPD) without being strongly influenced by neighboring pixels (i.e. negligible cross talk). No cross talk between pixels maximizes modulator resolution and simplifies wavefront control. In addition to increasing zero-order efficiency, the fill factor improvement increases power handling.

To obtain a large effective phase shift of several waves (or several hundred waves for steering beams), a LC SLM has to use modulo-2π modulation, which correctly wraps the phase pattern at only one wavelength. Therefore, an OPD SLM with limited stroke is dispersive when used with a broadband source. To increase the spectral operating range of LC SLMs, non-dispersive phase modulators using polarization rotation are being developed.[15] The use of the non-dispersive phase shifter coupled with an achromatic transformer provides broadband operation.[16] A visible system with achromatic operation over 400 nm to 800 nm has been demonstrated using limited-stroke modulators.[17] To provide a full wave of stroke, a high-tilt analog ferroelectric LC modulator is used.[18] Fortunately, the ferroelectric LC has sub-millisecond response, but it requires higher voltage addressing which limits backplane resolution. Therefore, the technique needs to be combined with coarse steering assemblies to provide wide field-of-view coverage. A broadband coarse steerer that provides 52° of steering[19] is discussed.

The enhancements mentioned above are best implemented using reflective mode-devices. With a reflective configuration, two passes through the modulator doubles the effect, allowing the LC modulator to be thinner. A thinner LC layer reduces response time and cross talk. Also, the double pass is needed for converting ±45° of tilt into a full wave of stroke or providing polarization-independent modulation using a single device.[20] In some applications, however, reflective configurations pose a problem, since optical systems are generally more compact using transmissive components.[21,22] This paper discusses some of the in-line configurations used to minimize the impact of using reflective devices in an optical assembly.

2. HIGH FILL FACTOR SLMS

The pixelation of a raw LCoS backplane, as shown in Figure 1, produces strong amplitude variations. Since little light is reflected from the inter-pixel spacing, the pixel gap represents a loss factor. However, this is not the only problem. The spatial variation causes the Fourier transform of the phase pattern produced by the SLM to be replicated at the harmonics associated with the pixel pitch. In some systems, these replicated patterns can be blocked and the diffraction is mostly an efficiency hit (power loss = 1 – (fill factor)^2). If the higher harmonics cannot be blocked, the pixelation produces artifacts that reduce image contrast or cause sidelobe interference. Therefore, it is desirable to maximize the output energy in the central replica (i.e. the zero-order). This output is maximized by:

1) making the pixel mirror fill the whole area to achieve a 100% fill factor, and
2) making as much of the mirror the same physical level (minimize optical phase variations).

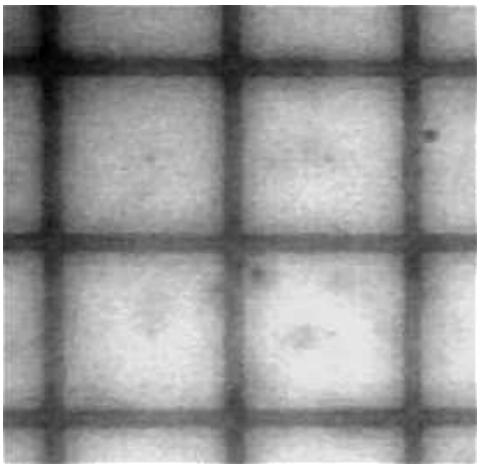

Figure 1: Pixelated LCoS SLM backplane.

Within the high-volume fabrication process of typical display backplanes, fill factor is normally maximized by using high-resolution lithography to keep the pixel gap small. With custom processing, dielectric coatings can be deposited onto planarized backplanes to achieve a nearly 100% flat fill factor (refer to Figure 2). Planarization removes most of the pixel-to-pixel topography and the dielectric mirror provides uniform reflectance over the surface of the backplane, hiding the electrode structure. The modified backplane acts as a continuous flat reflector with the incident light being affected only by the optical path difference (OPD) produced by the liquid crystal (LC) layer covering the mirror. The field that controls the OPD modulator is created by the pixel electrodes that are hidden by the dielectric stack. There are gaps between these electrodes, but the addressing fields spread to fill in the area between pixels as they traverse the modulator stack. This spreading smoothes the phase profile created by the modulator. Therefore, there is little dead space between pixels. However, the smoothing causes some cross talk between pixels, also.

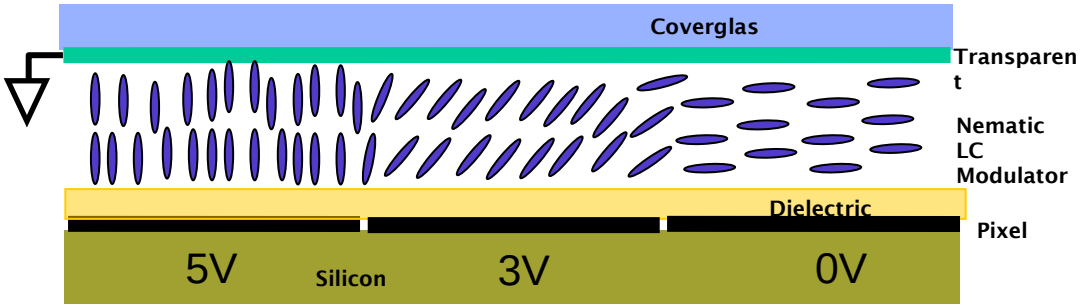

Figure 2: High throughput configuration for LCoS SLM.

The cross talk between pixels is a function of the modulator gap (i.e. the distance of the pixel electrode to coverglass electrode). This modulator gap with respect to the width of a pixel and the inter-pixel gap has a profound effect on the ability to convert the field at the electrode into a precise phase shift. The electric field smoothing, mentioned above, acts as a low pass filter causing discrete steps at each element to be smeared out spatially over a larger area. That is, there is some influence between pixels. This influence function makes the phase pattern more continuous and is beneficial when the phase variation is within the range of the LC modulator. Unfortunately, LC modulators have limited stroke and require modulo-2π operation to effectively produce large phase variations. With modulo-2π operation, the LC modulator needs to be abruptly reset where the phase pattern wraps. That is, the OPD changes by a full wave to retain pattern coherency. This abrupt change is prevented by the pixel-to-pixel influence producing an effect which is sometimes referred to as flyback.

Reduction of the flyback region is possible by using different material properties of liquid crystal. An obvious property that helps in this effort is the birefringence of the material. A highly birefringent material reduces the LC layer thickness needed to achieve 2π of phase modulation. Fortunately, there is very little down side to using the highest birefringence material available that meets device requirements. In addition to birefringence, other LC properties are useful for reducing the flyback effect, such as the elastic and electrical parameters of the material. These parameters affect the threshold voltage of the material.

For a parallel-aligned cell, the threshold voltage, V_{th}, is a function of the elastic constant, K_{11}, that keeps the molecules aligned parallel to the cell's surface and the difference, $\Delta\varepsilon$, in the perpendicular and parallel dielectric constants of the LC material as given by[23]

$$V_{th} = \pi\sqrt{K_{11} / \varepsilon_0 \Delta\varepsilon}\ , \tag{1}$$

where ε_o is the permittivity of free space.

At the threshold voltage, a small change in voltage produces a relatively large change in phase modulation as shown in Figure 3. This nonlinear transition is aided by using an alignment with no pre-tilt of the molecules. That is, all the long axes of the molecules are parallel with the surfaces of the cell. This arrangement reduces coupling to the field, keeping the molecules from rotating until the threshold voltage is exceeded. After it is exceeded, the bulk of the molecules rotate into the field producing a large change in retardance. This nonlinear optical response tends to counteract electrical smoothing and reduce the flyback region.

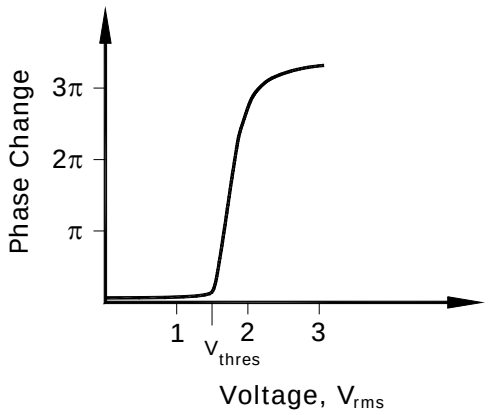

Figure 3: Response curve for a nematic parallel-aligned liquid crystal cell

If it is assumed that the field drops off linearly over a set distance, then the benefit of using the threshold effect to reduce flyback is easy to illustrate. The set distance is assumed to be equal to the gap between the pixel electrode and transparent electrode, which is approximately 5 microns for a 633 nm device. Because of the dielectric stack, a mirrored LCoS SLM operating at 633nm typically requires a 5-volt field to achieve a full wave of stroke. Therefore, a modulator, which has a 3-volt threshold, will restrict the flyback region to two microns. Where as, a modulator with a 1-volt threshold will have an extended flyback region of four microns. Within the flyback region, the intended phase pattern is disrupted, which causes the reflected light to be diffracted into undesirable sidelobes. Hence, a larger flyback results in less modulator efficiency and more sidelobe interference.

To keep flyback to a minimum, it is necessary to address the SLM with data that correctly localizes the modulo-2π phase wrap to two adjacent pixels. This localization requires the pixel array to capture voltage values that are specifically mapped to particular pixels. If there is not one-to-one mapping, due to sampling skew for example, the cross talk between pixels extends the flyback region over several pixels. Therefore, negligible cross talk maximizes modulator resolution and simplifies phase pattern generation (i.e. wavefront control).

In addition to increasing zero-order efficiency, the dielectric mirror improves power handling by blocking the light that causes photoconduction within the backplane. Without photoconduction depleting the addressing field, LCoS SLM power handling is greatly increased. The primary power handling issue then becomes one of heating. Heating is due to absorption with the major contributor being the transparent conductor on the coverglass. Transparent conductors with very little absorption have been developed, allowing LC SLMs to handle very high average power levels.[24]

3. BROADBAND OPERATION

By hiding the electrode structure under a dielectric stack, higher order diffraction is greatly reduced. However, this does not allow the SLM to correctly handle broadband light. The phase wraps produced by the OPD modulator are wavelength dependent. Thus, the phase pattern is only continuous at one design wavelength and broadband light is angularly dispersed by the discontinuous phase pattern. A key element for producing high-resolution, broadband dynamic wavefront control is a low dispersion spatial light modulator. Non-dispersive phase modulation with an analog modulation depth of up to 2π is achieved using the SLM configuration shown in Figure 4.

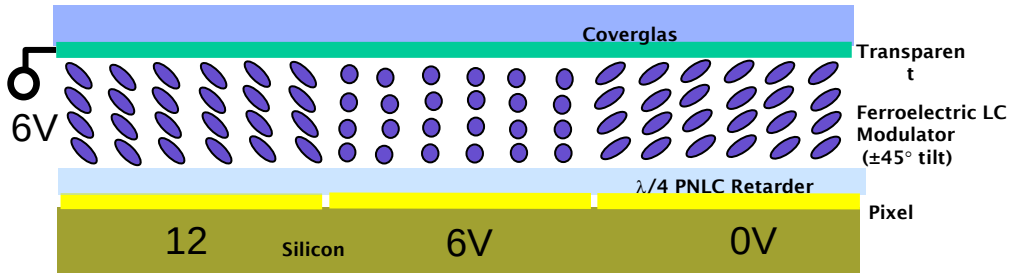

Figure 4: Non-dispersive, high-speed phase modulator configuration for LCoS SLM.

Figure 4 is cross section of LCoS SLM that uses optic axis reorientation to provide a topological (i.e. achromatic) phase shift. This modulator requires highly-reflective pixels and is optically flat over the area of the array. Above the mirrors is a passive quarter-wave retarder which preserves the handedness of the circularly polarized light incident on the modulator. This passive retarder is a polymer nematic liquid crystal (PNLC). A barrier layer separates the polymer LC from the active half-wave retarder. This barrier layer is a thin passivation that protects the solid nematic material from being dissolved by the ferroelectric liquid crystal (FLC) layer that is used for the active wave-plate.

The topological phase modulator design presented above requires a rotative half-wave FLC retarder. With an analog FLC modulator, sub-millisecond response is achievable from the SLM. However, the FLC retarder ideally should have a full molecular rotation angle of 90° to provide a full 2π phase shift. The molecular tilt is a function of the material being used. The only FLC that has sufficient tilt is a chiral smectic C (SmC*) material.

It is a common belief that SmC* materials are inappropriate for analog SLMs, because despite their large tilt angles and low voltage requirements, their switching tends to be binary in nature. However, it is now known and has been demonstrated that certain SmC* materials exhibit a controllable analog optical response[18] (refer to Figure 5).

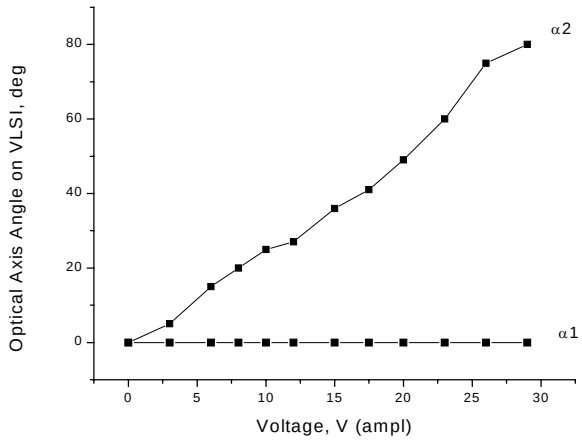

Figure 5: Optic axis orientation as a function of applied voltage at 1 Hz. Here the integrated modulator is configured to switch as a single pixel. Orientation of the optic axis relative to the zero field state is denoted by α1 or α2, each representing a different polarity.

Figure 5 is a plot of the optical response for a 1 Hz square wave applied to the integrated modulator. The integrated modulator consists of VLSI backplane, passive PNLC λ/4 retarder, active FLC λ/2 retarder and ITO-coated coverglass. The 78 degrees of optic axis reorientation translates to a phase modulation depth of 312 degrees. This is enough to implement 7 uniformly spaced quantized phase levels. The FLC used has a theoretical maximum reorientation of 86 degrees, but materials exist which can reorient by as much as 96 degrees.

Unfortunately, a non-dispersive phase shifter is not the only requirement for providing high-resolution wavefront control of a broadband source. The non-dispersive phase modulator only eliminates wavelength-dependent OPD problems. Since the configuration shown in Figure 4 provides a common phase shift for all wavelengths over a common distance, reflected broadband light is linearly dispersed by the modulator. To correct the angular dispersion, an achromatic Fourier transform (AFT) lens is needed.[25,26]

With an achromatic Fourier transform lens the grating dispersion is corrected causing the diffracted orders to be focused to a dot, as in Figures 6 (b) and 7 (b), instead of a dash, seen in Figures 6 (a) and 7 (a). The AFT is actually a lens system consisting of several elements. This lens system uses diffractive and refractive components to create different magnifications between common focal planes for the spectral components within broadband light. This wavelength-dependent scaling (or lateral color) eliminates the dispersion caused by the grating pattern and thus produces wavelength-independent spatial distributions for the transform. Figures 6 and 7 demonstrate that this arrangement operates as described.

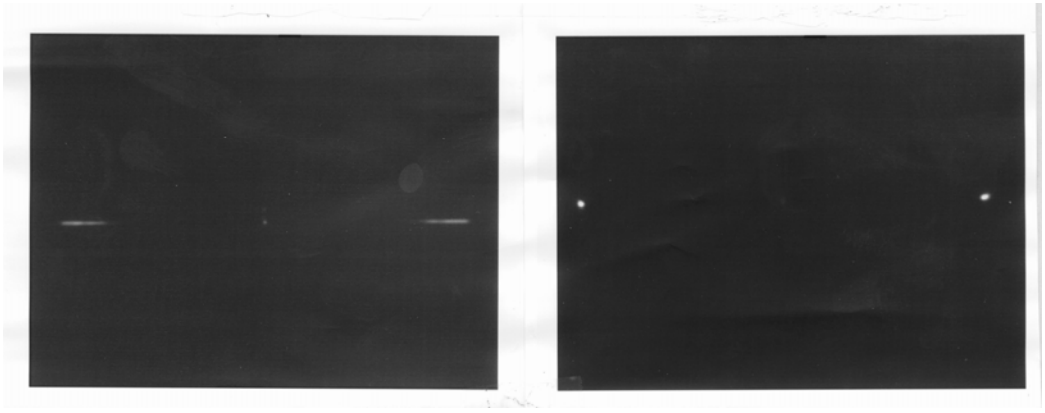

(a) (b)

Figure 6: Thermal prints of diffraction patterns created by non-dispersive SLM in a normal and AFT imaging system.

Figure 6 demonstrates that the FLC modulator produces a wavelength-independent phase shift, since the remnant central order is small even though the illumination is broadband, which is evident from the grating dispersion visible in the uncompensated diffracted orders (left side).

Figure 7 shows photographs of the dispersive and corrected far field diffraction patterns corresponding to a checker board pattern written to the SLM. These photos demonstrate that the AFT lens corrects grating dispersion regardless of azimuth. The checker board pattern is not perfectly symmetric, which results in a significant amount of undiffracted light in the zero order.

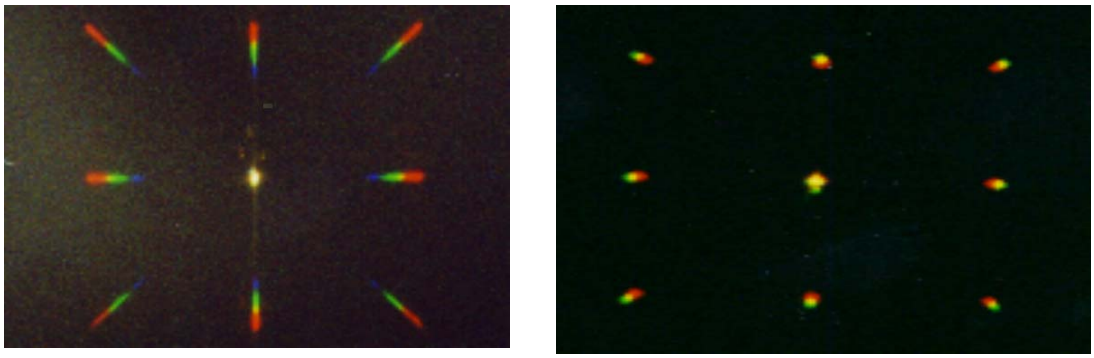

(a) (b)

Figure 7: Photographs of the far field patterns for a checker board written to the SLM. (a) Grating dispersion is present for a normal achromatic lens. (b) Grating dispersion has been corrected by the AFT lens.

The broadband technique described above provides high resolution correction, but its resolution is limited by backplane and modulator requirements. The modulator shown in Figure 4 requires higher voltage levels than those needed for standard nematic LC modulators. The voltage requirement increases the pixel pitch to accommodate the larger gate structures. For example, a high-voltage analog 256x256 backplane has been recently developed. The chip was fabricated through a 0.5-μm foundry process. The device has a pixel pitch of 24-μm with a flat fill factor of approximately 90%. This device provides 0 to 13 volts at the pixel which is still not enough voltage for the FLC modulator described by Figure 5. Larger gate structures do not significantly affect linear arrays, but have a large impact on two-dimensional arrays. Even without pixel pitch restrictions, the current modulator thickness is several microns, which prevents the device from exceeding a few degrees in steer angle due to flyback effects. To steer the field of view of a sensor over a large field of regard, a different approach is needed.

It is possible to change the field of view of a sensor by changing its focal plane position. As shown in Figure 8, plane waves from different directions are focused to different spots at the focal plane of a lens. Due to reciprocity, focused beams launched from different spots within the focal plane of a lens will be angularly tilted based on the launch position of the beam. The angle depends on the speed of the lens (i.e. f/#) and the X and Y displacement of the focal plane position from the lens' optical axis. The maximum displacement from the optical axis is half the lens diameter (for half-power operation). Therefore, the maximum steer angle is given by

$$\theta_{max} = \tan^{-1} [1/(2\ f/\#)]. \qquad (2)$$

A technique for non-mechanically translating the focal plane position has been developed. The translation is performed by a 2-D assembly which physically repositions the focal point of the image through a series of internal reflections. Each bounce through the structure translates the focal spot a discrete amount. The incident light is re-imaged after each bounce. A liquid crystal switch at each discrete focal plane location determines if the light will be released from the structure, or forced to propagate to the next discrete location. The structure therefore acts as a coarse steerer. The number of discrete locations needed is a function of the desired field-of-view and the total field of regard set by the lens f-number.

The technique for non-mechanically shifting the spot within the focal plane is shown in Figure 9. The focus translator uses a highly reflective mirror and a reflective wire-grid polarizer to walk the spot in one

direction using multiple bounces between the two reflective components. On each bounce, the beam travels through a relay lens, which re-images the beam at the focal plane of the steering lens. It is the relay lens that keeps the spot in focus at the focal plane of the steering lens as the beam is routed to different zones. A transmissive LC shutter array controls the routing and launching of the beam at the desired location. Each pixel acts as a polarization rotator, allowing the beam's polarization to be controlled with applied voltage. The polarization induced at each LC cell determines if the beam is launched (if parallel to the polarizer) or reflected back into the reflecting structure (if polarized perpendicular to the polarizer).

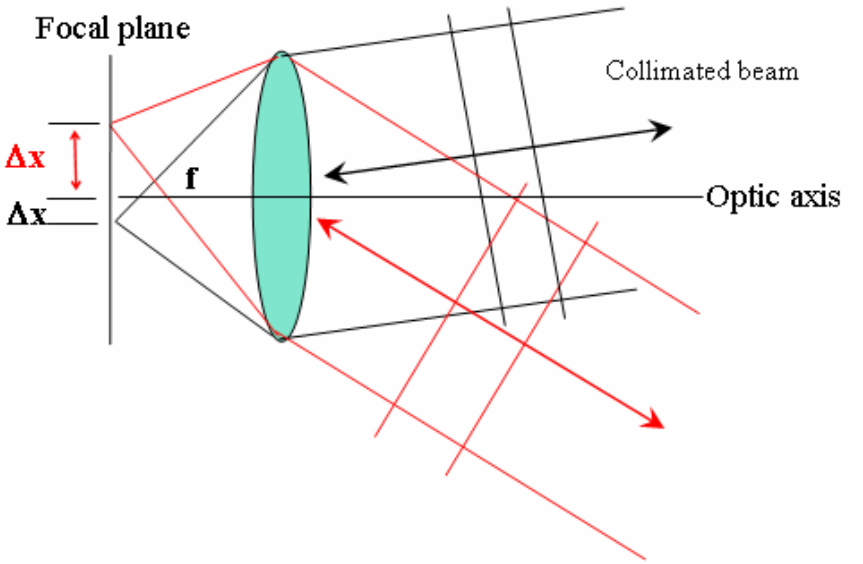

Figure 8: Basic concept for wide angle approach.

Figure 9 shows the beam being routed in one direction. In this example, the beam enters the router at the top of the focal plane and walks to the bottom through several bounces. If a pixel is activated, the liquid crystal rotates the beam's polarization, allowing some or the entire beam to pass through the wire-grid polarizer. This manipulation of the polarization causes the beam to be launched (transmitted) or passed to the next pixel. Due to reciprocity, the reverse occurs when a beam is received. A received beam, entering the steering lens from a specific angle, is focused to a spot at a particular location in the focal plane. The focused beam, having the proper polarization, passes through the wire-grid polarizer (orthogonally polarized light is reflected by the polarizer). If the pixel at that location is activated, then the light's polarization is rotated, and the beam walks to the top of the focal plane, exiting the router to propagate along the optic axis of the system. At a non-activated pixel, a focused beam enters through the polarizer. However, its polarization remains unchanged and passes back through the polarizer on the first bounce, leaving the system.

For two-dimensional (2D) steering, a second linear translation stage is needed to walk the beam horizontally after the beam is brought to the desired vertical location. A 2D arrangement is shown in Figure 10. As the beam is routed to a new position, it loses some energy on each bounce. This loss needs to be minimized to make the system practical for use in laser communications, laser radar or IR imaging applications. By index matching the components and using highly reflective mirrors and wire-grid polarizers, the loss on each bounce is minimized. However, there is then a need to minimize the number of bounces required to translate the beam. That is, the coarseness of the beamsteerer needs to be maximized for any application. To provide coverage in azimuth and elevation over 50°x50° in 10°x10° steps using the configuration shown in Figure 8, the coarse steering stage segments the focal plane of the steering lens (f/# = 1) into an array of 5x5 zones. Therefore, the maximum number of steps needed to translate the beam to any position is 10, which according to a recent demonstration effort is not an excessive number of bounces.

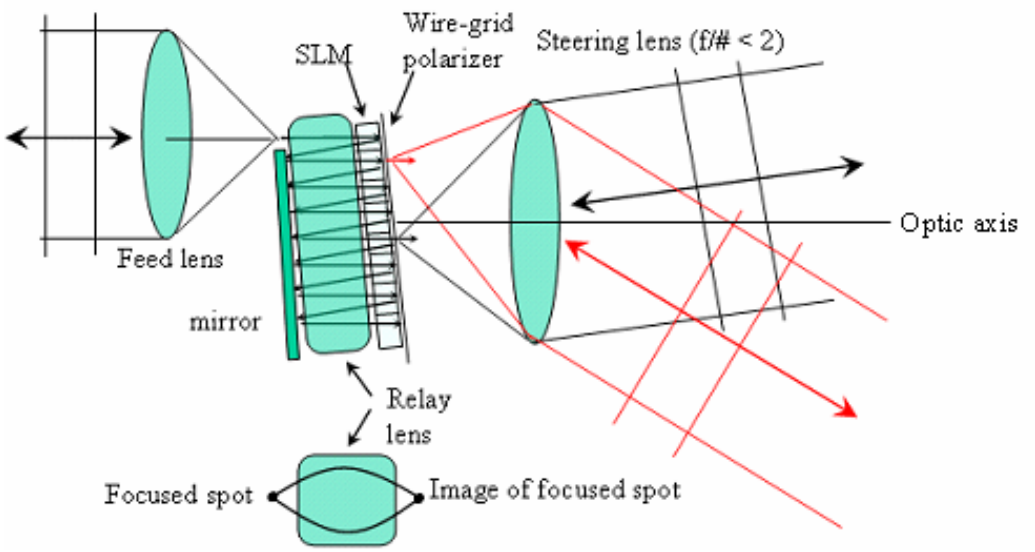

Figure 9: One-dimensional coarse steerer.

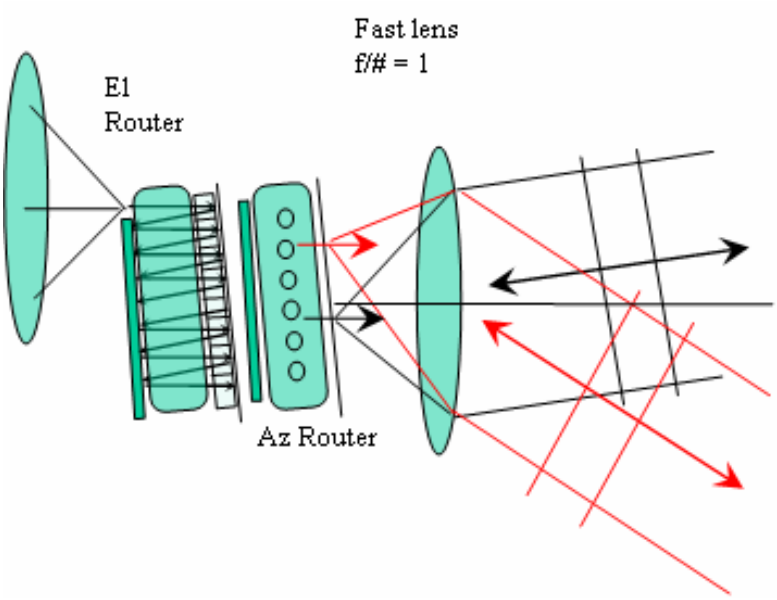

Figure 10: Two-dimensional coarse steering stages.

Recently, the feasibility of the coarse stepper concept was proven through a visible wavelength demonstration. For the demonstration system, the focal plane translator used a White cell configuration, which consists of two parabolic reflectors that translate and refocus the beam at the focal plane of a fast lens (f/#=1). A 1x32 twisted nematic shutter array was used to select the steer angle. The coarse stepper assembly steered a laser beam over a ±26° field of regard. Figure 11 shows the demonstration system steering over the wide field of regard.

This technique uses refractive components to steer the beam to large angles allowing non-dispersive (broadband) steering. Even though a linear array is used to steer the beam, it only acts as a shutter. It does not use a limited stroke modulator to add a high-resolution phase pattern to the beam. The phase tilt occurs when the focal plane position is converted by the fast lens into an angular direction. Fortunately, the fast

lens is also the exit aperture, keeping this broadband beam from having the same walkoff problems that are associated with other coarse steering approaches. Beam walkoff forces the physical size of the beam steering assembly to grow to accommodate less aperture efficiency.

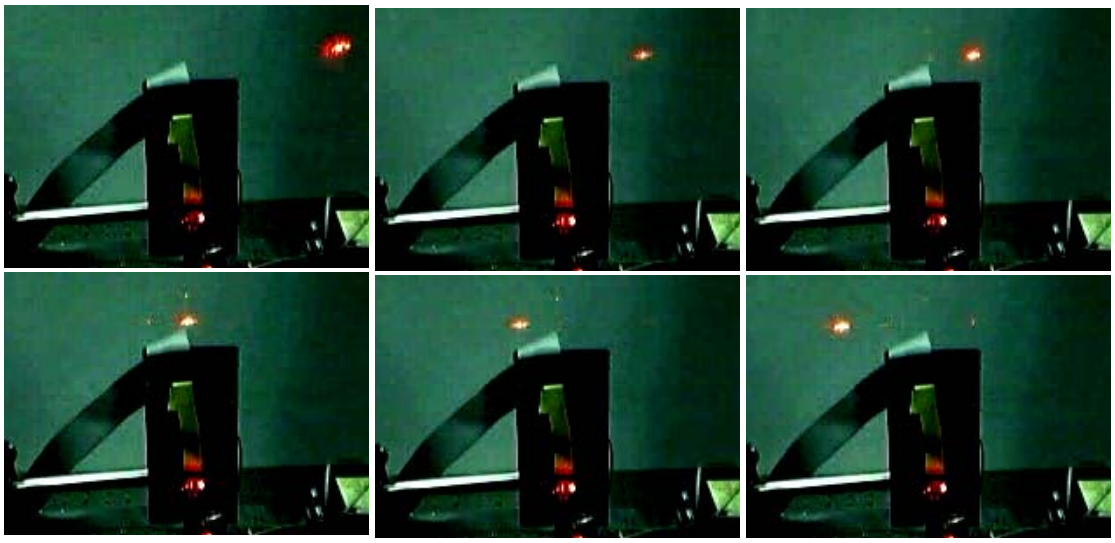

Figure 11: A visible demonstration of the coarse stepper concept.

4. COMPACT CONFIGURATIONS

The reflective modulators shown in Figures 2 and 4 offer several improvements over the current state of the art. These modulator configurations reduce diffraction and provide broadband operation. What is missing is a compact reflective configuration that does not add significantly to the size and weight of the optical system over a transmissive arrangement. This problem is being addressed for a few different applications where in-line operation significantly simplifies the optical system.

One possible in-line configuration is shown in Figure 12. The foveated imaging system provides well-corrected images over a wide field of view (FOV) using a relatively simple optical lens system and SLMs to correct the image at desired locations. It uses a high-index (n = 2.28) Pechan prism to help compress the FOV and route the light onto two reflective 2D LCoS SLMs. With two SLMs, two separate wavelength bands or two orthogonal polarizations can be independently processed, which provides a 3 dB improvement over using a single LCoS device. By increasing the index of the prism assembly, the FOV is increased without modifying the lens design, which is possible using silicon (n = 3.5 to 3.4) in the near IR and mid-wave IR, respectively.

Another in-line configuration using reflective devices is shown in Figure 13. Multiple optical phased arrays (OPAs) are phased together to act as a common aperture forming a phased array of phased arrays (PAPA). Figure 13 shows a fiber array feeding a stack of OPA devices. Light from each fiber strikes a reflective OPA device on the top of a "louver" orientated at 45 degrees to the source. The light then travels up to a second reflective OPA device mounted on the bottom of a "louver", and then exits the device. Each top/bottom OPA pair reproduces a transmissive optical element capable of 2D (conical) scanning when the OPA backplanes are properly oriented to provide azimuth and elevation steering.

A 3x3 PAPA system was recently demonstrated.[27] The system coherently combined and steered nine beams from separate fiber feeds over a ±1.5° field of regard using nine 1x4096 LCoS OPAs. In addition to demonstrating that the beam profile from a properly phased aperture was maintained while the system

steered to different angles, it showed that a very compact in-line configuration was possible, benefiting from low-power and lightweight LCoS components to form larger apertures with size, weight and power advantages over traditional gimbal approaches.

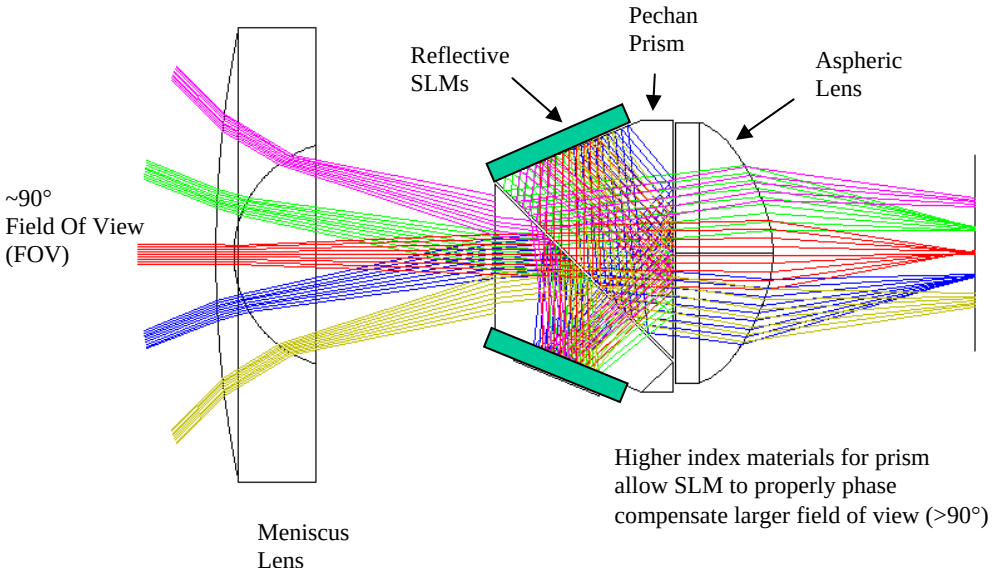

Figure 12: Modeling results from a foveated imaging system using reflective SLMs as the wavefront controller. The imaging system has a ±45° FOV. The corresponding ZEMAX™-generated ray traces show that only the center traces are in focus. SLM-aided correction is required to bring other areas into focus.

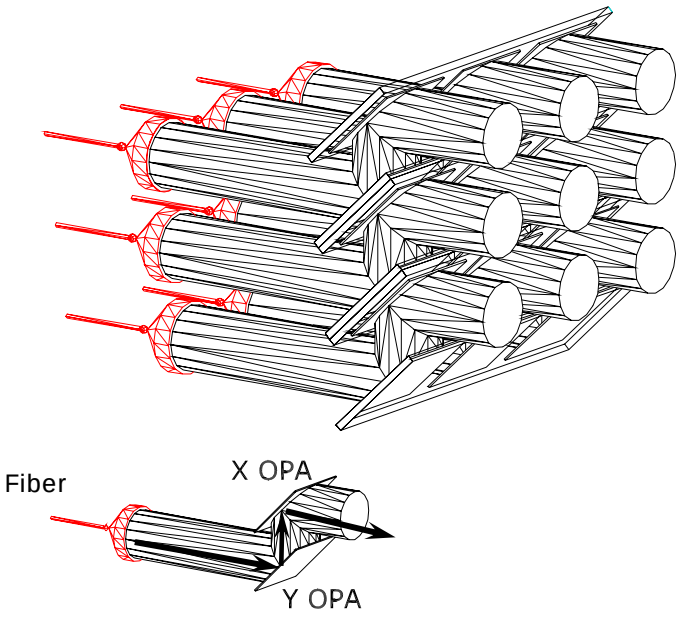

Figure 13: Phased array of LCoS optical phased arrays.

5. CONCLUSIONS

Based on recent developments:

- Zero-order efficiency of LCoS SLMs can be better than 90%,
- Power handling is limited by the absorption of the transparent conductor which can be reduced to allow the LCoS SLM to operate with average power levels of hundreds of watts per square centimeter,
- Cross talk can be minimized by correctly using LC material parameters,
- Broadband wavefront control and wide field of regard steering is possible using sub-millisecond modulators,
- Compact, in-line configurations for minimizing the size and weight of the optical system can be achieved using reflective modulators that offer the above advancements.

These improvements extend the capability of the LCoS SLM technology making the devices suited for a variety of applications.

ACKNOWLEDGEMENTS

The work presented in this paper includes contributions from Hugh Masterson, Anna Linnenberger, Jamie Harriman and Teresa Ewing.

REFERENCES

[1] P.F. McManamon, E.A. Watson, T.A. Dorschner and L.J. Barnes, "Applications look at the use of liquid crystal writable gratings for steering passive radiation," *Opt. Eng*., vol. **32**, no. 11, pp. 2657-2664, (Nov. 1993)

[2] E. Watson, P. McManamon, L. Barnes and A. Carney, "Application of dynamic gratings to broad spectral band beam steering," *SPIE*., **Vol. 2120**, (1994).

[3] McManamon *et.al.*, "Optical Phased Array Technology," Proceedings of the IEEE, Vol. **84**, No. 2, (Feb. 1996).

[4] S. Serati and J. Stockley, "Phased Array of Phased Arrays (PAPA) for Free Space Optical Communications," 2003 IEEE Aerospace Conference, **5**, paper – 5.0502 (March 2003).

[5] J. Stockley, S. Serati, X. Xun, R. W. Cohn, "Liquid crystal spatial light modulator for multispot beam steering," Proc. SPIE, **5160**, pp. 208-215 (2004).

[6] D.G. Grier, "A revolution in optical manipulation," Nature, **424**, 810-816 (2003).

[7] X. Xun, X. Chang, D.J. Cho, and R.W. Cohn, "Arbitrary multi-beam laser scanning and trapping by use of a spatial light modulator and manual scripting interface," Proc. SPIE, **5514**, pp. 143-149 (2004).

[8] C.H.J. Schmitz, J.E. Curtis, and J.P. Spatz, "Constructing and probing biomimetic models of the actin cortex with holographic optical tweezers," Proc. SPIE, **5514**, pp. 446-454 (2004).

[9] S. Restaino *et. al*., "Use of electro-optical device for path-length compensation," Proc. SPIE **2200**, pp. 46-48 (1994).

[10] R.S. Dou and M.K. Giles, "Closed loop adaptive optics system with a liquid-crystal television as a phase retarder," Opt. Lett. **20**, 1583-1585 (1995).

[11] G.D. Love, "Wavefront correction of Zernike modes with a liquid crystal spatial light modulator," Appl. Opt. **36**, 1517-1524 (1997).

[12] M.T. Gruneisen, T. Martinez and D.L. Lubin, "Dynamic Holography for High-Dynamic-Range Two-Dimensional Laser Wavefront Control," Proc. SPIE, **4493**, pp. 224-238 (2002).

[13] M.K. Giles, A. Seward, M.A. Vorontsov, J. Rha, and R. Jimenez, "Setting up a liquid crystal phase screen to simulate atmospheric turbulence," Proc. SPIE, **4124**, pp. 89-97 (2000).

[14] M.R. Brooks and M.E. Goda, "Atmospheric simulation using a liquid crystal wavefront controlling device," Proc. SPIE, **5553**, pp. 258-268 (2004).

[15] K. Bauchert, S. Serati and A. Furman, "Advances in liquid crystal spatial light modulators," in *Optical Pattern Recognition XIII, Proc. SPIE,* **Vol. 4734**, (2002).
[16] J. Stockley, S. Serati, G. Sharp, P. Wang, K. Walsh and K. Johnson, "Broad-band Beam Steering," *Proc. Of SPIE*, **Vol. 3131**, (1997).
[17] J. Stockley, S. Serati, D. Subacius, K.J. McIntyre, and K.F. Walsh, "Broadband phase-modulating system for white-light Fourier transformations," *Proc. SPIE*, **3633,** pp. 196-205 (Jun 1999).
[18] J.E. Stockley, *Chiral Smectic Liquid Crystal Beam Deflector with Large Analog Phase Modulation*, Ph.D. Thesis – University of Colorado, (1996).
[19] S. Serati and J. Stockley, "Nonmechanical Wavelength-independent Beam Steerer," U. S. Patent Application Publication No. US 2005/0007668 filed July 11, (2003).
[20] G.D. Love, "Liquid-crystal phase modulator for unpolarized light," *Applied Optics*, **Vol. 32**, No. 13, May 1, (1993).
[21] T. Martinez, D.V. Wick, and S.R. Restaino, *Optics Express* **8**, 555-560 (2001).
[22] D.V. Wick, T. Martinez, S.R. Restaino, and B.R. Stone, "Foveated imaging demonstration," *Optics Express* **10**, 60-65 (2002).
[23]I.C. Khoo and S.T. Wu, *Optics and Nonlinear Optics of Liquid Crystals,* Singapore: World Scientific Publishing Co. (1993).
[24] J. Perkins, C. Teplin, M. van Hest, C. Warmsingh, D. Ginley, and S. Harris,"Optimization of Transparent Conducting Oxides for Liquid Crystal Based Optical Phased Arrays", *Proc. 2003 IEEE Aerospace Conference*, **4**, 5.0801, p. 4-1823, (2003).
[25] R. Katyl, "Compensating Optical Systems – Part 3: Achromatic Fourier Transformation," *Appl. Opt.*, **Vol. 11**, pp.1255-1260 (1972).
[26] G. Morris, "Diffraction theory for an achromatic Fourier transformation," *Appl. Opt.*, **Vol. 20**, No. 11, (1981).
[27] S. Serati, H. Masterson and A. Linnenberger, "Beam combining using a Phased Array of Phased Arrays (PAPA)," 2004 IEEE Aerospace Conference, **5**, paper – 5.0205 (Mar 2004).